AFRL-AFOSR-UK-TR-2011-0043

# CONTROL OF SPATIALLY INHOMOGENEOUS SHEAR FLOWS

**Dan S. Henningson**
**Reza Dadfar**
**Onofrio Semeraro**
**Shervin Bagheri**
**Luca Brandt**

**KTH The Royal Institute of Technology**
**Department of Mechanics**
**Stockholm, Sweden S-100 44**

EOARD SPC 10-4006

October 2011

Final Report for 21 September 2010 to 21 September 2011



**Air Force Research Laboratory**
**Air Force Office of Scientific Research**
**European Office of Aerospace Research and Development**
**Unit 4515 Box 14, APO AE 09421**

# REPORT DOCUMENTATION PAGE

Form Approved OMB No. 0704-0188



| 1. REPORT DATE *(DD-MM-YYYY)* | 2. REPORT TYPE | 3. DATES COVERED *(From – To)* |
|---|---|---|
| 06-10-2011 | Final Report | 21 September 2010 – 21 September 2011 |

**4. TITLE AND SUBTITLE**

**CONTROL OF SPATIALLY INHOMOGENEOUS SHEAR FLOWS**

**5a. CONTRACT NUMBER**

FA8655-10-M-4006

**5b. GRANT NUMBER**

SPC 10-4006

**5c. PROGRAM ELEMENT NUMBER**

**6. AUTHOR(S)**

**Professor Dan S Henningson**
**Reza Dadfar**
**Onofrio Semeraro**
**Shervin Bagheri**
**Luca Brandt**

**5d. PROJECT NUMBER**

**5d. TASK NUMBER**

**5e. WORK UNIT NUMBER**

**7. PERFORMING ORGANIZATION NAME(S) AND ADDRESS(ES)**

KTH The Royal Institute of Technology
Department of Mechanics
Stockholm, Sweden S-100 44

**8. PERFORMING ORGANIZATION REPORT NUMBER**

N/A

**9. SPONSORING/MONITORING AGENCY NAME(S) AND ADDRESS(ES)**

EOARD
Unit 4515 BOX 14
APO AE 09421

**10. SPONSOR/MONITOR'S ACRONYM(S)**

AFRL/AFOSR/RSW (EOARD)

**11. SPONSOR/MONITOR'S REPORT NUMBER(S)**

**AFRL-AFOSR-UK-TR-2011-0043**

**12. DISTRIBUTION/AVAILABILITY STATEMENT**

Approved for public release; distribution is unlimited. (approval given by local Public Affairs Office)

**13. SUPPLEMENTARY NOTES**

**14. ABSTRACT**

It was demonstrated the possibility to delay the transition process using a feedback controller based on localized sensors/actuators. Three-dimensional TS wave packets and streaks with finite amplitudes are considered; reduced-order models based on balanced truncation are built and used for the control design. The controller mitigates the disturbances amplitude when the flow is still laminar but nonlinear, resulting in a significant reduction of the perturbation energy and, later, in a delay of the transition process. The robustness of the device is tested by varying the controller effort. A too strong controller effort resulted in a worsening of the performance when the TS scenario is considered: this behavior of the device is in contrast with the linear prediction. This effect is due to the excitation of higher order harmonics, related to the three-dimensionality of the controller action, combined to the nonlinearities of the uncontrolled flow. Conversely, the controller built for streaks is less affected by the nonlinearities of the flow; indeed, for this case, the localization is able to mimic the spatial distribution of the incoming disturbance. The resulting actuation is not introducing additional disturbances of smaller scale and the only nonlinearities are those characterizing the uncontrolled flow. Starting from this knowledge, a further improvement of the device can be achieved by explicitly accounting for the nonlinear effects during the modeling process when needed. Moreover, modern developments in robust control theory may be used to rigorously incorporate uncertainties that may be present in the design process.

**15. SUBJECT TERMS**

EOARD, Aerodyanamics, Control System

| 16. SECURITY CLASSIFICATION OF: | | | 17. LIMITATION OF ABSTRACT | 18, NUMBER OF PAGES | 19a. NAME OF RESPONSIBLE PERSON |
|---|---|---|---|---|---|
| a. REPORT | b. ABSTRACT | c. THIS PAGE | | | Gregg Abate |
| UNCLAS | UNCLAS | UNCLAS | SAR | 13 | 19b. TELEPHONE NUMBER *(Include area code)* +44 (0)1895 616021 |

# Control of Spatially Inhomogeneous Shear Flows

*EOARD Grant SPC 8655-10-M-4006*

Reza Dadfar, Onofrio Semeraro, Shervin Bagheri, Luca Brandt, Dan S. Henningson
Linné Flow Centre, KTH Mechanics, Stockholm, Sweden

In this EOARD/AFOSR project, we aim at combining state-of the-art numerical simulations and advanced methods in control theory to significantly reduce drag over bodies, such as the wing of an airplane. In particular, our objective is to suppress the growth of small-amplitude disturbances to delay the point on the wing surface where the flow becomes turbulent, thus decreasing the overall drag.

The research efforts in the field of feedback flow control at Linné Flow Centre, KTH Mechanics, led by Prof Dan Henningson, have been partially supported through the EOARD Grant FA 8655-07-1-3053. Besides the project leader, Prof. Henningson, two graduate students will be involved in this continuation project, Onofrio Semeraro (3rd year) and Reza Dadfar (1st year), one assistant professor Dr. Shervin Bagheri and one associate professor, Dr. Luca Brandt.

Since we introduced a framework (so-called input-output approach) based on low-dimensional models, localized sensors and actuators and optimal/robust feedback control [3, 1], significant progress (for a recent summary see [2]) has been made in controller development for the attenuation of small-amplitude disturbances inside a spatially developing boundary layer. Low-dimensional models of fully three-dimensional, multi-actuator-multi-sensor open-loop systems have been successfully constructed, characterized, and used to design efficient feedback controllers to delay transition to turbulence [4]. In particular, it was found that the growth of disturbances typically encountered in the presence of low and moderate free-stream turbulence can be reduced - thus transition to turbulence delayed- using a few (of order 10) spatially localized sensors and actuators distributed near wall (see attached paper soon to be submitted to the *Journal of Fluid Mechanics*).

More recently, the focus of the project has been on improving the modeling of actuators, sensors and disturbances to increase experimentally feasibility and – on a shorter perspective – to reveal fundamental performance and control limitations present in transition control. The plasma actuator has received considerable attention over the past several years as viable candidate for transition control due to its localized nature and ability to generate momentum forcing (without fluidic plumbing), which makes it attractive and relatively straight-forward to model numerically. In the same spirit, we are systematically investigating the optimal number of placement of sensors (mimicking wall hot wires) and increasing the complexity of the geometry, by including an elliptic leading edge in both two-dimensional and three-dimensional setups.

Our most recent results show that using the framework based on localized sensors and actuators and optimal feedback control we can efficiently reduce growth of disturbances inside a boundary layer, when they are generated (for example by harmonic forcing) in the free-stream upstream of an elliptic leading edge of a flat-plate. Moreover, we have designed models of dielectric barrier discharge (DBD) plasma-actuators, where a comparison between simulation and experimental results is underway. Although the preliminary results are very promising, the use of plasma actuators necessities the design of a more advanced controller that can handle the constraints introduced by the actuator.

# References

[1] S. Bagheri, L. Brandt, and D. S. Henningson. Input-output analysis, model reduction and control design of the flat-plate boundary layer. *J. Fluid Mech.*, 620:263–298, 2009.

[2] S. Bagheri and D. S. Henningson. Transition delay using control theory. *Phil. Trans. R. Soc. A*, 369:1365–1381, 2011.

[3] S. Bagheri, J. Hœpffner, P. J. Schmid, and D. S. Henningson. Input-output analysis and control design applied to a linear model of spatially developing flows. *Appl. Mech. Rev.*, 62(2), 2009.

[4] O. Semeraro, S. Bagheri, L. Brandt, and D. S. Henningson. Feedback control of three-dimensional optimal disturbances using reduced-order models. J. Fluid Mech. (Published online 30 Mar 2011), 2011.

# Transition delay in a boundary layer flow using feedback control

**ONOFRIO SEMERARO, SHERVIN BAGHERI, LUCA BRANDT AND DAN S. HENNINGSON**

Linné Flow Centre, KTH Mechanics, SE-100 44 Stockholm, Sweden

(Received 10 May 2011)

Feedback control is applied to delay the onset of laminar-turbulent transition in a boundary-layer over a flat plate. Two different three-dimensional localized initial conditions – a Tollmien-Schlichting and a streak wavepacket – with finite amplitudes are used to numerically simulate the transition to turbulence. Using the same framework of Semeraro *et al.* (2011), linear controllers based on reduced-order models of the linearised Navier-Stokes equations, are connected to sensors and actuators localized near the wall. It is shown that using this linear control approach, the onset of laminar-turbulent transition can be delayed at least by$\Delta\ Re_x \approx 2 - 3 \times 10^5$ for both the transition scenarios. Effect of the actuation on the disturbances and the effort of the controller are characterized in the nonlinear regime.

**Key Words:**

## 1. Introduction

This paper considers the control of laminar-turbulent transition in the flat-plate boundary layer triggered by the growth and breakdown of finite-amplitude three-dimensional disturbances. In clean environments characterized by low levels ($T_u < 1\%$) of free-stream turbulence (FST), nearly two-dimensional Tollmien–Schlichting (TS) wavepackets are often observed in the boundary layer. The amplitude of these perturbations (initially of order 1% of the free-stream velocity) grows at an exponential rate, which after a temporal sequence of events eventually leads to a turbulent flow. This scenario is referred to as the classical route to transition. A different scenario – bypass transition – observed for higher values of FST ($T_u > 1\%$), is characterized by the presence of three-dimensional streaks. The amplitude of these streamwise elongated structures grows at an algebraic rate, but are approximately one order of magnitude larger than TS waves. From a technological point of view it is of interest to control these routes to transition in order to reduce drag, which in turn may lead to significant savings, for instance, in the operational cost of cargo ships or commercial aircraft.

A general input-output framework for feedback control was developed in Bagheri *et al.* (2009*a*), where the disturbance and actuators were considered as inputs, and the objective function and sensors were considered as outputs. The approach is based on approximating the complex high-dimensional system that arises from discretization of the Navier-Stokes equations with a low-order model (see Bagheri & Henningson 2011, for a recent review). Using approximate balanced truncation (Rowley 2005), a low-order system preserving the dynamics between the actuators and sensors is developed, followed by the design of the controller. Semeraro *et al.* (2011) extended the analysis to a fully three-dimensional

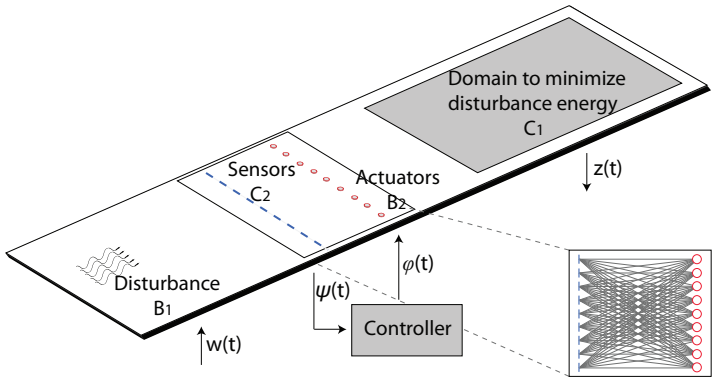


FIGURE 1. Sketch of the control configuration employed for delaying the onset of transition to turbulence. The disturbance ($\mathbf{B}_1$) consists of an optimal initial condition. A spanwise row of sensors ($\mathbf{C}_2$) are connected via an LQG low-order controller to a row of actuators ($\mathbf{B}_2$). The objective of the controller is to minimize the disturbance energy in the region spanned by the leading 10 POD modes (marked with the gray color). The inset figure shows that all the sensors are wired to all the actuators (so-called centralized control).

(3D) configuration and demonstrated that the perturbation energy can be substantially mitigated using localized actuation and sensing; in this latest work, the control setup was based on a set of localized actuators and sensors distributed near the wall resembling actual experimental setups (see *e.g.* Sturzebecher & Nitsche 2003; Lundell 2007).

Although successful, these previous investigations considered perturbations of such low amplitude to be governed by linearised equations. In this work we employ the configuration introduced in Semeraro *et al.* (2011) to examine the effect of linear feedback control in the full nonlinear regime with finite-amplitude perturbations leading to transition to turbulence. We show under which conditions the control results in a delay of the initial stages of the laminar-turbulent transition. We also investigate the effects of a strong actuation on the flow for high disturbance amplitudes.

## 2. Overview of configuration and numerical method

The governing equations of finite-amplitude perturbations in a viscous, incompressible flow over a flat plate and the modelling of actuators and sensors are presented in this section. The velocity field is denoted with $\overline{\mathbf{u}}(\mathbf{x},t) = (\overline{u},\overline{v},\overline{w})^T$ and is governed by the Navier–Stokes equations; $x$, $y$ and $z$ denote the streamwise, wall-normal and spanwise coordinates, respectively. The Reynolds number is defined as $Re_{\delta_0^*} = U_\infty \delta_0^*/\nu$, where $\delta_0^*$ is the displacement thickness at the inflow position, $U_\infty$ is the uniform free-stream velocity and $\nu$ is the kinematic viscosity. We choose $Re_{\delta_0^*} = 1000$, corresponding to $Re_x \approx 3 \times 10^5$ at the computational inlet. The simulations presented in this paper were performed using a pseudo-spectral direct numerical simulation (DNS) code (Chevalier *et al.* 2007). Dirichlet conditions enforce zero perturbations velocity in the free-stream ($y = L_y$) and at the wall ($y = 0$). Periodicity is assumed in the spanwise direction and enforced in the streamwise direction by a fringe region at the outlet of the domain.

Large eddy simulations (LES) were performed using the ADM-RT subgrid-scale model for the simulation of transition. Schlatter *et al.* (2004) showed that ADM-RT model is accurate and robust in predicting transitional and turbulent flows with spectral methods. Note, however, that the subgrid-scale model (SGS) term is effectively active only when the

| | Resolution | Box | Cases | Penalty $l$ | Tran. delay $\Delta x$ | Reynolds Num. $\Delta Re_x$ |
|---|---|---|---|---|---|---|
| Streaks | $1024 \times 101 \times 256$ | $[1000, 30, 128]$ | A | 50 | $\approx$295 | $3.0 \times 10^5$ |
| | | | B | 100 | $\approx$330 | $3.3 \times 10^5$ |
| | | | C | 200 | $\approx$265 | $2.7 \times 10^5$ |
| TS waves | $1536 \times 101 \times 256$ | $[2000, 30, 256]$ | D | 200 | $\approx$100 | $1.0 \times 10^5$ |
| | | | E | 250 | $\approx$180 | $1.8 \times 10^5$ |
| | | | F | 300 | $\approx$220 | $2.2 \times 10^5$ |

TABLE 1. Test cases for the analysis of the transition delay; the parameter used is the control penalty $l$. The performance is compared considering the achieved transition delay in terms of $\Delta x$ and$\Delta$ $Re_x$.

flow becomes turbulent. An application of LES in flow control, using the same numerical method, is discussed by Monokrousos *et al.* (2008), where comparisons with full DNS are carried out. In section 3, we report our results for six different configurations (labeled A-F in table 1). In all cases the LES resolution was deemed sufficient for obtaining converged results and verified using DNS.

### 2.1. *Input-output system and control design*

The control strategy employed in Semeraro *et al.* (2011) to control 3D disturbances with infinitesimal amplitude is also used in the present investigations for finite-amplitude perturbations. For consistency we briefly describe the linear control system; the reader is referred to Semeraro *et al.* (2011) for a more detailed description and an in-depth discussion.

The first step is the linearization of the Navier-Stokes equations around a steady state $\mathbf{U}(\mathbf{x}, t) = (U(x, y), V(x, y), 0)$. Representing the inputs with $\mathbf{B}_1$ and $\mathbf{B}_2$, and the outputs with $\mathbf{C}_1$ and $\mathbf{C}_2$, a linear state-space system is written as

$$\dot{\mathbf{u}}(t) = \mathbf{A}\mathbf{u}(t) + \mathbf{B}_1\mathsf{w}(t) + \mathbf{B}_2\phi(t) \tag{2.1a}$$

$$\mathsf{z}(t) = \mathbf{C}_1\mathbf{u}(t) + I_l\phi(t) \tag{2.1b}$$

$$\psi(t) = \mathbf{C}_2\mathbf{u}(t) + I_\eta\mathsf{g}(t), \tag{2.1c}$$

where $\mathbf{A}$ is obtained from the discretization of the linearised Navier-Stokes including the boundary conditions and $\mathbf{u} = (u, v, w)$ is the perturbation velocity field. A sketch of the configuration is provided in figure 1.

The disturbance is introduced upstream by a localized initial condition $\mathbf{B}_1$, providing the maximum energy growth of the perturbation at a given final time (see Monokrousos *et al.* 2010). The second input $\mathbf{B}_2$ consists of an array of localized actuators described by an analytical Gaussian function. The temporal forcing of the system is provided by the input signals $\mathsf{w}$, $\mathsf{g}$ and $\phi$, which model, respectively, the temporal behavior of disturbance $\mathbf{B}_1$, the presence of noise in the measurements and the control signal feeding the actuators.

The output signal $\psi(t)$ is extracted by an array of localized sensors $\mathbf{C}_2$, which are located a short distance upstream of the actuators and aligned with them. The level of white noise contamination of the measurement is accounted by the constant vector $I_\eta$.

Lastly, the output signal $\mathsf{z}(t)$ is used to assess the performance of the controller. The signal is obtained by projecting the velocity field on a sequence of 10 proper orthogonal decomposition (POD) modes. The modes are generated by a dataset of snapshots col-

lected from the impulse response to the initial condition $\mathbf{B}_1$ and are represented by the columns of $\mathbf{C}_1$. The entries of the matrix $I_l$ represent the effort of the controller: large values indicate higher control costs and therefore weaker actuation. The norm of $\mathsf{z}(t)$ represents the objective function of our system (Bagheri *et al.* 2009*a*).

A reduced-order model allows us to easily access the tools of linear control theory. For our application, a basis of approximate balanced modes (Rowley 2005) is computed using a snapshot-based method. A set composed by 60 modes was deemed sufficient for accurately reconstructing the linear input-output behaviour of the system. The controller is designed using the linear quadratic Gaussian (LQG) approach (see *e.g.* Dullerud & Paganini 1999; Bagheri *et al.* 2009*b*) and is of the same low order as the model. The spatial localization of the actuators and the sensors requires a proper multi-input-multi-output (MIMO) approach for the controller design, where all actuators are connected to all sensors (centralized control). This configuration results in a stable closed-loop system.

## 3. Transition delay

As mentioned previously, the classical transition scenario is usually observed in the presence of low FST and is triggered by the growth of TS wavepackets; when higher levels of FST are considered, transition is promoted by the lift-up mechanism and is related to the appearance of streamwise streaks. The two scenarios can be initiated by introducing initial conditions that in a linear framework experience the largest possible amplification at a final time. We define the amplitude of a disturbance by,

$$a = \left( \max_{x,y,z} u - \min_{x,y,z} u \right) / 2U_\infty. \tag{3.1}$$

The localization of the actuators and sensors, the control penalties and the initial amplitudes – already introduced – provide a broad range of parameters to be examined. In the present study, a parametric analysis is carried by varying the penalty $l$, while the configuration of actuators and sensors and the noise contamination, $\eta = 0.01$, are fixed. In particular, the controller designed for the streaks is characterized by 8 actuators and 8 sensors, whereas the controller designed for the TS-wave consists of 9 elements for each array. The chosen configurations showed the best performance in the linear simulations (Semeraro *et al.* 2011).

### 3.1. *Transition delay of streaks*

Figure 2*a* shows the kinetic energy of a disturbance with initial amplitude of $a = 0.05\%$ and (linearly) optimized for short final time. After approximately 350 time units – when the disturbance is located at $Re_x = 6.5 \times 10^5$ and has an amplitude of $a \approx 25\%$ – an abrupt increase of energy growth rate is observed as the streak breaks down and rapidly develops into a turbulent spot. When the control is active, the sudden increase in energy growth rate is observed at $t \approx 700$ as shown by the black line in figure 2*a*. Before the streak develops into a turbulent spot it has a propagation velocity $c_{le} = 0.90$ (see Monokrousos *et al.* 2010). Using this value, the transition delay is estimated to$\Delta\, x = 330$ and$\Delta\, Re_x = 3.3 \times 10^5$, which is significant increase in distance along the plate.

To gain insight into how the controller modifies the perturbation, the streamwise velocity of the streaks are shown in figures 2($b-e$) with and without control at two different time instants. The comparison of the streaky structures at $t = 300$ shows that the flow structure is essentially left unmodified by the action of the controller; however, the amplitude of disturbance is reduced by approximately$\Delta\, a \approx 9\%$. This mitigation leads to a delay of the transition to turbulence; indeed, the perturbation structure is still laminar at

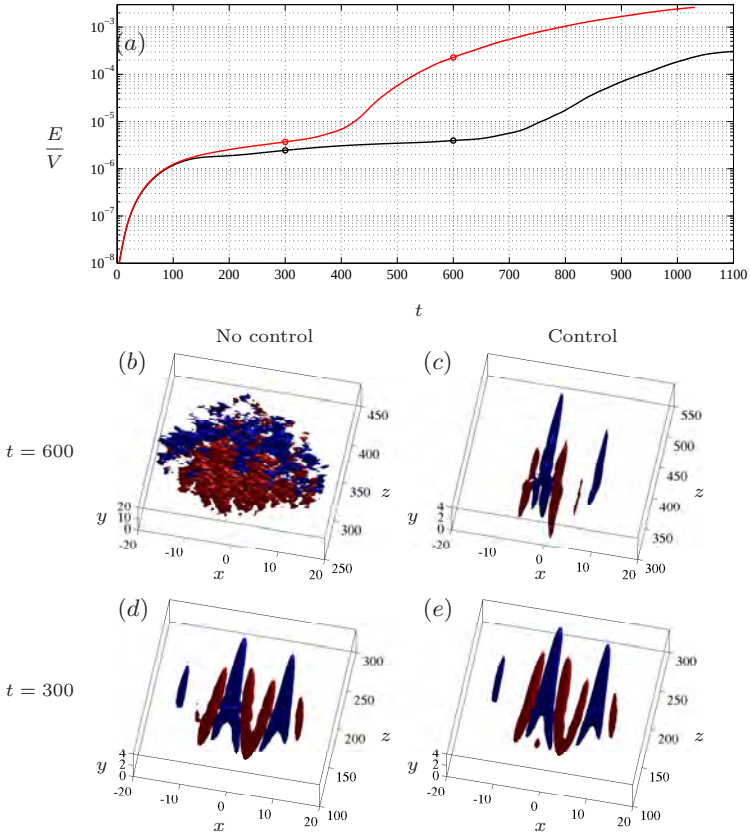


FIGURE 2. In (a) the red line depicts the evolution of the energy-density of a streak, whereas the black line shows the same quantity when feedback control (case B in table 1) is applied. Frames (b)-(e) show instantaneous (at $t = 300$ and $t = 600$) contour plots of 30% of the maximum of the streamwise velocity component of the streak for the both the uncontrolled configuration (left frame) and the controlled one (right frame).

$t = 600$ when the control is active, while the uncontrolled flow developed into a turbulent spot.

In table 1, the transition delay in terms of$\Delta\ x$ and$\Delta\ Re_x$ are shown for different values of the control penalty $l$ corresponding to cases A-C. In all cases, transition delay is achieved but the best performance is obtained for $l = 100$. When $l$ is larger (case C) the control cost is more expensive and less reduction in perturbation energy is achieved. On the other hand, when $l$ is smaller (case A) control cost is cheaper, but it results in a too strong forcing which quickly triggers nonlinear effects – dynamics which the controller is not designed to take into account.

### 3.2. *Transition delay of TS waves*

To achieve transition delay in the presence of TS wavepackets, a longer computational box is required so that the controller can be active when the flow is still laminar. Also, a much wider box would be appropriate since the TS wavepacket spreads in the spanwise direction rapidly as it propagates downstream. In the present configuration, the disturbance interacts with itself due to the limited spanwise width of the computational box, but this interaction is downstream of the position of the actuators.

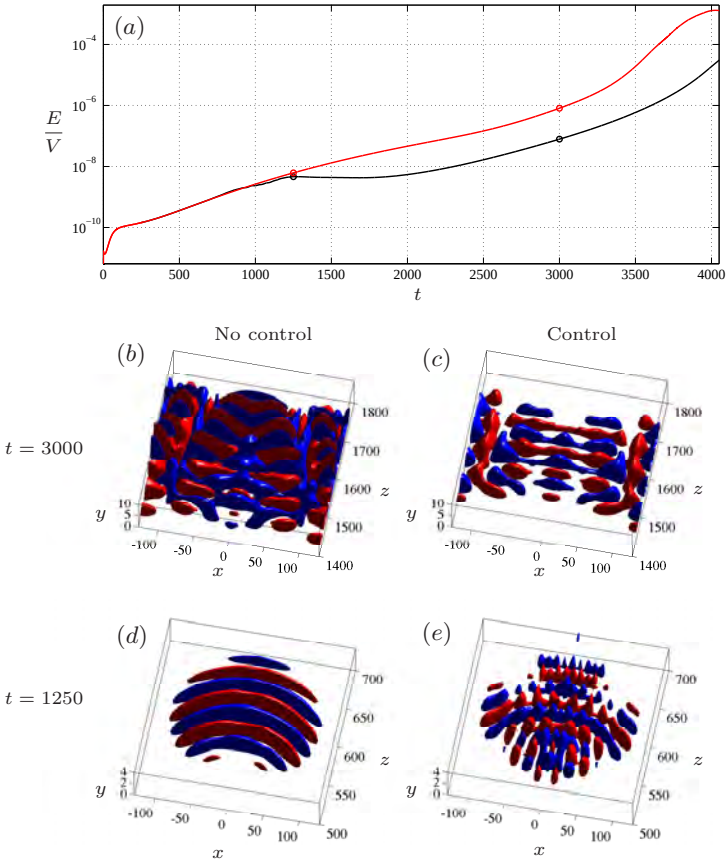


FIGURE 3. In (a) the red line depicts the evolution of the energy-density of a TS wavepacket, whereas the black line shows the same quantity when feedback control (case F in table 1) is applied. Here the energy is scaled with the total volume of the computational domain. Frames (b)-(e) show instantaneous (at $t = 1250$ and $t = 3000$) contour plots of 30% of the maximum of the streamwise velocity component of the streak for the both the uncontrolled configuration (left frame) and the controlled one (right frame).

Figure 3$a$ (red line) shows the time evolution of the energy of a TS wavepacket of initial amplitude $a = 0.03\%$. The initial condition is nearly two-dimensional and is tilted in the upstream direction. First, the disturbance extracts energy from the mean flow via the Orr-mechanism resulting in a very rapid growth. This is followed by an exponential growth until the disturbance breaks down to a fully three-dimensional structure, where higher wavenumbers are quickly triggered; later in time, a turbulent spot is observed in the computational box. In the same figure, the energy curve when control is active is shown with a black line. The disturbance reaches the array of actuators after approximately 1000 time units, the perturbation energy is damped by roughly an order of magnitude; note that the arrays of actuators and sensors are placed further downstream compared to the configuration employed for the streaks. Since the action of the controller is limited only to a nearby region of the actuators, the perturbation begins to grow further downstream and eventually triggers transition.

Comparing the spatial structures of the disturbance with and without control in figures 3$(b-d)$, we observe that the controller changes the actual structure of the perturbation – a fundamental difference to the streak configuration. Due to the localization of the

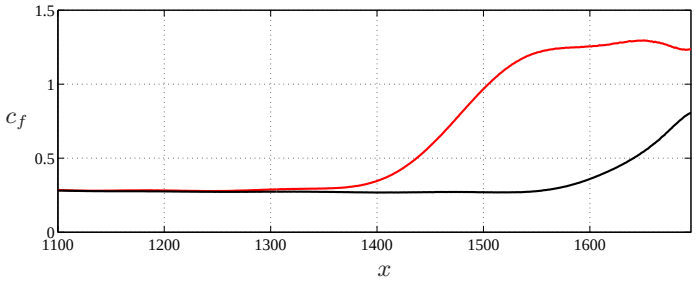


FIGURE 4. The skin friction coefficient $c_f$ versus the streamwise direction for a TS wavepacket without control (red line) and with control (black line) corresponding to case F in table 1.

actuators and their equidistant placement in the spanwise direction, the original nearly 2D wavepacket is sliced into a more complicated 3D structure as it traverses the actuators. In a purely linear analysis a 3D wavepacket is less unstable (i.e. has a smaller growth rate), but in a nonlinear regime it requires a lower threshold to trigger turbulence. To achieve transition delay, it is therefore essential that the controller acts in the linear regime of the transition process. In fact, careful inspection of the flow fields shows that this is the case for the chosen parameters: downstream of the actuation array, the perturbation gradually recovers its spanwise coherence, which leads to renewed growth of a the TS-wavepacket. Note that the slope of the energy curve for the controlled perturbation is essentially the same as for the uncontrolled case (see black line figure 3*a*).

The skin friction coefficient $c_f$ as a function of the downstream distance is shown in figure 4, where the sudden increase of $c_f$ indicate the onset of transition. We observe that transition is delayed by approximately$\Delta\ x = 220$, corresponding to $Re_x \approx 2.2 \times 10^5$.

In table 1, the control performance in terms of transition delay is reported when the control penalty is varied. It is interesting to note the transition delay increases with the control cost. This is in contrast to a linear setting, where a smaller control cost results in a better control performance. The opposite trend with respect to $l$ can again be attributed to that high actuation amplitudes may trigger nonlinear effects more quickly than low amplitudes.

## 4. Analysis of the controlled flow

In this section, a more thorough analysis of the actuation is performed considering energy spectra and amplitude expansions. Figure 5 shows the energy spectrum of the streak perturbation at $t = 400$ in the $\alpha - \beta$ plane, where $\alpha = 2\pi N_x/L_x$ is the streamwise wavenumber and $\beta = 2\pi N_z/L_z$ the spanwise wavenumber of the perturbation. The excitation of harmonics of the fundamental streak wavenumber, $\beta \approx 0.6$, is evident for the uncontrolled flow (figure 5*a*). The spectrum of the controlled perturbation (figure 5*a*) is, apart from minor adjustments, essentially left unmodified when the actuators are switched on. In other words, the controller does not introduce any new wavenumbers in the flow, which would trigger additional new nonlinear effects. The resulting controlled flow is characterized by the same wavenumbers as the original flow, only with a lower energy content.

From this point of view, the TS scenario is different and more complicated; indeed, in this case, the three dimensionality (i.e. the localized spanwise arrangement of the actuators) of the controller introduces new disturbances in the field. In order to analyse the main features of the controlled and uncontrolled flow, we perform an amplitude

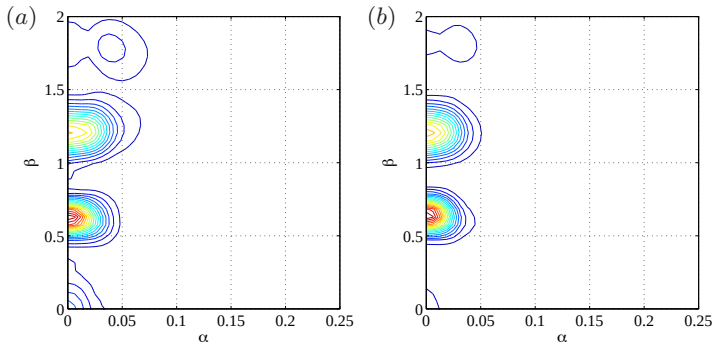


FIGURE 5. Streak: energy spectra at $t = 400$ for the uncontrolled case ($a$) and the controlled case ($b$). The isocontour levels are 19 and the peak is normalized versus the maximum amplitude. In particular, the controlled case is characterized by a peak in energy $\approx 17\%$ smaller than the uncontrolled case.

expansion of the flow field at a given time (figure 6), where the following expansion is applied to the perturbation velocity

$$\mathbf{u}(\epsilon) = \sum_{k=1}^{n} \mathbf{u}_k \epsilon^k + O\left(\epsilon^{n+1}\right). \tag{4.1}$$

Here, $\epsilon$ represents the initial amplitudes, $\mathbf{u}_k$ the perturbation velocity fields, and $n = 3$ for our application. The first order, $n = 1$, corresponds to the linear solution, while $n > 1$ indicates perturbations triggered by nonlinear interactions. The $\mathbf{u}_k$ components are computed from velocity fields obtained with several values of $\epsilon$ in (4.1); we refer to Henningson *et al.* (1993) for more details.

First, the uncontrolled flow is considered at $t = 1000$ (see figure $6a-c$). The quadratic nonlinear interaction, $n = 2$, introduces structures elongated in the streamwise direction and characterized by $\beta \approx 0.1$. At the third order, the energy peak is obtained from the interaction between the linear term and the quadratic term. The corresponding controlled case is reported in figure $6(d-f)$. As discussed in the previous section, we confirm that the three-dimensionality of the control action introduces new wavenumbers characteristic of the controller. Indeed, the spectrum of the first order term (figure $6d$) in the expansion shows a clear damping of the energy at the frequency related to the TS-waves and the appearance of 3D modes due to the localization of the actuation. The quadratic term is characterized by two peaks at $\beta \approx 0.1$ (figure $6e$); the first is characterized by a lower value of $\alpha$ and is related to the nonlinearities of the uncontrolled flow. The second peak is related to the interaction between the action of the controller and the uncontrolled flow and is found also in the cubic term (figure $6f$). Moreover, it is observed that in the nonlinear terms $n > 1$, higher-order spanwise modes $\beta > 0.2$ appear. Thus, the propagation of energy to smaller spanwise scales appears to be due to the interaction between the controller and the uncontrolled flow. This worsens the performance of the controller for larger amplitudes of the initial disturbance and reduces the robustness of the controller when a stronger controller effort is introduced. Although TS wave have lower amplitudes than streaks, the actuation introduces secondary instability modes. Indeed, we observe that for larger amplitudes of the incoming TS, localized actuation promotes the transition to turbulence. Note that the controller is based on the linearised Navier–Stokes equations and therefore nonlinear interactions are not included. Nonlinear effects

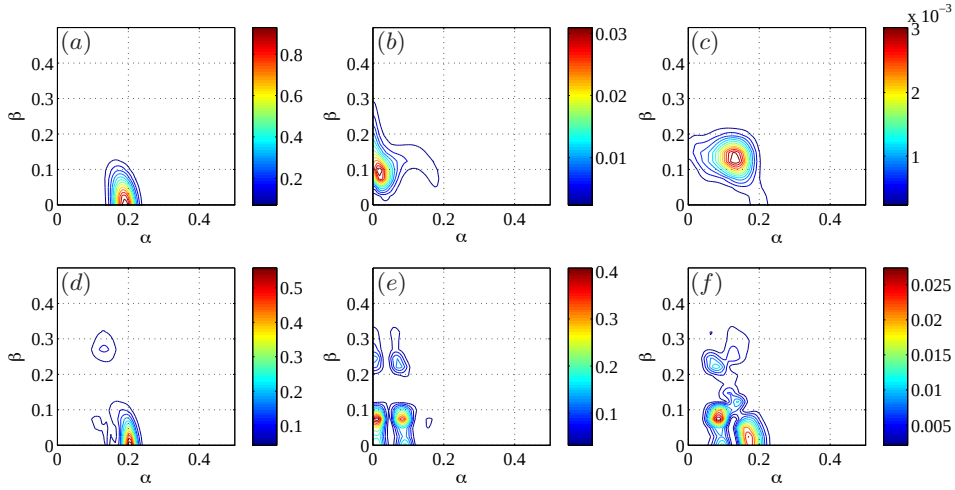


FIGURE 6. TS waves: Amplitude expansion analysis at $t = 1000$ for the uncontrolled case. The energy spectra are shown for the first $(a)$, the second $(b)$ and third order $(c)$; the corresponding controlled case is shown in $d - f$. The contour level are normalized to the maximum level in $a$.

need to be included in the reduced order modeling in order to increase the performance of the controller.

## 5. Conclusion

We demonstrated the possibility to delay the transition process using a feedback controller based on localized sensors/actuators. Three-dimensional TS wavepackets and streaks with finite amplitudes are considered; reduced-order models based on balanced truncation are built and used for the control design. The controller mitigates the disturbances amplitude when the flow is still laminar but nonlinear, resulting in a significant reduction of the perturbation energy and - later - in a delay of the transition process.

The robustness of the device is tested by varying the controller effort. A too strong controller effort resulted in a worsening of the performance when the TS scenario is considered: this behaviour of the device is in contrast with the linear prediction. This effect is due to the excitation of higher order harmonics – related to the three-dimensionality of the controller action – combined to the nonlinearities of the uncontrolled flow.

Conversely, the controller built for streaks is less affected by the nonlinearities of the flow; indeed, for this case, the localization is able to mimic the spatial distribution of the incoming disturbance. The resulting actuation is not introducing additional disturbances of smaller scale and the only nonlinearities are those characterizing the uncontrolled flow.

Starting from this knowledge, a further improvement of the device can be achieved by explicitly accounting for the nonlinear effects during the modeling process when needed. Moreover, modern developments in robust control theory may be used to rigorously incorporate uncertainties that may be present in the design process.

This work was partially sponsored by the Air Force Office of Scientific Research, through the European Office EOARD, under grant/contract number FA8655-10-M-4006. Computer time provided by SNIC (Swedish National Infrastructure for Computing) and financial support from the Swedish Research Council (VR) are gratefully acknowledged.

## REFERENCES

Bagheri, S., Brandt, L. & Henningson, D. S. 2009*a* Input-output analysis, model reduction and control design of the flat-plate boundary layer. *J. Fluid Mech.* **620**, 263–298.

Bagheri, S. & Henningson, D. S. 2011 Transition delay using control theory. *Phil. Trans. R. Soc. A* **369**, 1365–1381.

Bagheri, S., Hœpffner, J., Schmid, P. J. & Henningson, D. S. 2009*b* Input-output analysis and control design applied to a linear model of spatially developing flows. *Appl. Mech. Rev.* **62** (2).

Chevalier, M., Schlatter, P., Lundbladh, A. & Henningson, D. S. 2007 A pseudo spectral solver for incompressible boundary layer flows. Trita-Mek 7. KTH Mechanics, Stockholm, Sweden.

Dullerud, E. G. & Paganini, F. 1999 *A course in robust control theory. A convex approach*. Springer Verlag, New York.

Henningson, D. S., Lundbladh, A. & Johansson, A. V. 1993 A mechanism for bypass transition from localized disturbances in wall-bounded shear flows. *J. Fluid Mech.* **250**, 169–207.

Lundell, F. 2007 Reactive control of transition induced by free-stream turbulence: an experimental demonstration. *J. Fluid Mech.* **585**, 41–71.

Monokrousos, A., Åkervik, E., Brandt, L. & Henningson, D. S. 2010 Global optimal disturbances in the Blasius boundary-layer flow using time-steppers. *J. Fluid Mech.* **650**, 181–214.

Monokrousos, A., Brandt, L., Schlatter, P. & Henningson, D. S. 2008 DNS and LES of estimation and control of transition in boundary layers subject to free-stream turbulence. *Int. J. Heat Fluid Flow* **29** (3), 841–855.

Rowley, C. W. 2005 Model reduction for fluids using balanced proper orthogonal decomposition. *Int. J. Bifurc. Chaos* **15** (3), 997–1013.

Schlatter, P., Stolz, S. & Kleiser, L. 2004 LES of transitional flows using the approximate deconvolution model. *Int. J. Heat Fluid Flow* **25** (3), 549–558.

Semeraro, O., Bagheri, S., Brandt, L. & Henningson, D. S. 2011 Feedback control of three-dimensional optimal disturbances using reduced-order models. Firstview article (Published online), DOI: 10.1017/S0022112011000620.

Sturzebecher, D. & Nitsche, W. 2003 Active cancellation of Tollmien–Schlichting waves instabilities on a wing using multi-channel sensor actuator systems. *Int. J. Heat Fluid Flow* **24**, 572–583.